

S9.4b

Trimetallic Cu-Zn-Fe nanoparticles induced apoptosis and cell cycle arrest in multidrug-resistant *Candida auris*

S9.4 Free oral presentations (late breaking), September 23, 2022, 4:45 PM - 6:15 PM

Hammad Alam¹, Aijaz Ahmad^{1,2*}¹Clinical Microbiology and Infectious Diseases, Faculty of Health Sciences, School of Pathology, University of the Witwatersrand, Johannesburg 2193, South Africa²Infection Control Unit, Charlotte Maxeke Johannesburg Academic Hospital, National Health Laboratory Service, Johannesburg 2193, South Africa.

Background: *Candida* species are opportunistic fungus that can cause serious infections, particularly in immunocompromised population. The number of fungal infections has increased steadily with *Candida* species being responsible for > 70% of these instances, particularly in hospitalized patients with significant underlying conditions. Pharmacological resistance in *Candida* species and the advent of *Candida auris* have elevated candidiasis to a major public health concern. *Candida auris* is an emerging multidrug-resistant fungus that can cause catastrophic bloodstream infections and high fatality rates, particularly in hospitalized patients with major medical issues. Antifungal study of trimetallic nanoparticles (NPs) of various types have been studied as a therapy option for efficient and safe control of candidiasis. These NPs were highlighted for being environmentally friendly and sustainable synthetic preparative possibilities.

Objective: This work aimed to synthesize and characterize novel Cu-Zn-Fe trimetallic NPs and determine their *in vitro* antifungal activity and mechanism of antifungal action against *Candida auris* isolates.

Methods: The synthesis and characterization of Cu-Zn-Fe trimetallic NPs was done by standard methods. The antifungal capability of these NPs were determined by calculating minimum inhibitory concentrations (MIC) and minimum fungicidal concentrations (MFC) following CLSI recommended guidelines. Susceptibility on planktonic cells and biofilms was further confirmed by MuscTM cell count and viability assay and scanning electron microscopy (SEM) respectively. For insight antifungal mechanisms, apoptosis and cell cycle arrest were studied by exploring different apoptotic markers and MuscTM cell analyzer.

Results: Characterizations by Fourier-transform infrared spectroscopy (FTIR), diffuse reflectance UV-visible spectroscopy, X-ray diffraction (XRD), scanning electron microscopy (SEM), and transmission electron microscopy (TEM) determine the successful biosynthesis of Cu-Zn-Fe trimetallic NPs. Susceptibility assay confirmed the fungicidal activity of Cu-Zn-Fe NPs with MIC and MFC values of 12.5 and 25 µg/ml respectively. These results were further confirmed by viability assay reporting the cell viability of 45.5%, 13.5%, and 1.8% when *C. auris* cells were treated with 1/2 MIC, MIC, and 2MIC respectively. Cell cycle analysis revealed that 91.2% of healthy developing untreated control cells were in G0/G1 phase, whereas 5.2% and 3.7% of cells were in the S phase and G2/M phase, respectively. In contrast, NP-treated cells were observed to be arrested in S phase with 49.3% cells at 2MIC. To study the physiology of cell death caused by NPs, we investigated mitochondrial membrane potential (Δψ_m), with live cells having stable (Δψ_m) whereas treated cells showed loss of (Δψ_m). Another important parameter of apoptosis in yeast cells is the release of cytochrome C from the mitochondria to the cytosol and NP-treated cells resulting in decreased mitochondrial cytochrome C and elevated cytosolic cytochrome C levels. Both results confirmed the potential test NPs in causing apoptotic cell death in *C. auris*.

Conclusion: The trimetallic (Cu-Zn-Fe) nanoparticles displayed strong antifungal activity against *C. auris*, with a potential to arrest the cell cycle at S-phase, which could be linked to the DNA damage. Important yeast apoptotic markers suggested that the test NPs have a potential to cause apoptosis in *C. auris*. All these findings suggest the potential of these trimetallic NPs to be taken to the next level of research in the development of novel antifungal medications.

S9.4c

Diverse environmental inputs mediate changes in β-glucan exposure at the *Candida albicans* cell surface thereby influencing tissue colonisation during systemic infectionArnav Pradhan¹, Qinxin Ma¹, Emer Hicks¹, Gabriela Avelar², Daniel Larcombe¹, Judith Bain², Delma Childers², Ivy Dambuzza¹, Ian Leaves¹, Leandro Jose de Assis¹, Mihai Netea^{3,4}, Gordon Brown¹, Lars Erwig^{5,6}, Neil A. R. Gow¹, Ailistair J. P. Brown¹¹MRC Centre for Medical Mycology, University of Exeter, Exeter, United Kingdom²Institute of Medical Science, University of Aberdeen, Aberdeen, United Kingdom³Department of Internal Medicine and Radboud Centre for Infectious Diseases, Radboud University Medical Centre, Nijmegen, Netherlands⁴Department for Immunology & Metabolism, Life and Medical Sciences Institute (LIMES), University of Bonn, Bonn, Germany, ⁵Johnson-Johnson Innovation, EMEA Innovation Centre, One Chapel Place, London, United Kingdom

S9.4 Free oral presentations (late breaking), September 23, 2022, 4:45 PM - 6:15 PM

Candida albicans adaptation to host niches affects the exposure of key pathogen-associated molecular patterns (PAMPs) on its cell surface and, consequently, the detection of *C. albicans* cells by the immune system. Focusing on β-(1,3)-glucan, we screened for host inputs that influence the exposure of this immune-stimulatory PAMP on the *C. albicans* cell surface. We used a combination of fluorescent microscopy, flow cytometry, and cytokine assays, and then analyzed certain conditions in more detail using transmission electron microscopy and time-lapse video microscopy of *C. albicans*-phagocyte interactions. We found that some nutrients, micronutrient limitation, stresses, and antifungal drugs trigger β-glucan masking, whereas other inputs, such as nitrogen sources and quorum sensing molecules, exert limited effects on β-glucan exposure. In particular, host or bacterial-derived L-lactate, hypoxia, or iron limitation induce β-glucan masking, and this leads to attenuation of phagocytic responses [Nature Micro 2, 16 238; mBio 9, e01318-18; Nature Comms 10, 5315]. Lactate signals through Gpr1 to activate Crz1 in a calcineurin-independent manner, whereas hypoxia signals via mitochondrial ROS, and iron limitation signals through Ftr1 and Set1. β-glucan masking also depends upon downstream signaling via the cAMP-PKA pathway. We conclude that *C. albicans* has evolved to exploit a range of specific host-derived signals to modulate the exposure of a major PAMP at its cell surface in an attempt to evade phagocytic uptake. Using barcode-sequencing in direct competition assays *in vivo*, we showed that preadaptation to specific β-glucan masking signals affects the ability of this fungus to colonize particular tissues during systemic infection in a murine model. This reinforces the view that β-glucan masking promotes *C. albicans* infection.

S9.4d

Main reservoirs of *Trichophyton mentagrophytes* Type V in IranSivash Nikkholgh¹, Ivan Pchelint², Ali Zarei Mahmoudabadi¹, Mahbubeh Shabanzadeh-Bardar¹, Maral Gharaghani³, Aghil Sharifzadeh⁴, Rasoul Mohammadi⁵, Sadegh Noripour-Sisakht⁶, Farzad Katiraee⁶, Ali Rezaei-matehkolaei¹¹Infectious and Tropical Diseases Research Center, Health Research Institute, Ahvaz Jundishapur University of Medical Sciences, Ahvaz 61357-15794, Iran, Ahvaz, Iran²Institute of Experimental Medicine, 197 022 Saint Petersburg, Academician Pavlov St. 12, Russia, Saint Petersburg, Russia³Medicinal Plants Research Center, Yasuj University of Medical Sciences, Yasuj 75919-94799, Iran, Yasuj, Iran⁴Department of Microbiology and Immunology, Faculty of Veterinary Medicine, University of Tehran, Tehran, Iran, Tehran, Iran⁵Department of Medical Parasitology and Mycology, School of Medicine, Infectious Diseases and Tropical Medicine Research Center, Isfahan University of Medical Sciences, Isfahan 81746-73461, Iran, Isfahan, Iran⁶Department of Pathobiology, Faculty of Veterinary Medicine, University of Tabriz, Tabriz 51666-16471, Iran, Tabriz, Iran

S9.4 Skin mycoses and microbiome, September 23, 2022, 4:45 PM - 6:15 PM

Objectives: Dermatophytosis in livestock receives attention because of its contagiousness, high treatment costs, and lack of control programs. Compared with cattle, mycological aspects of dermatophytosis in sheep and goats have been studied less frequently. Dermatophytosis in these animals (small ruminants) may lead to serious economic losses due to the negative impact on the growth of involved animals, as well as their milk and meat production. Recent studies showed that the old *Trichophyton verrucosum* var. *verrucosum* (which is known to have some African and Asiatic sheep as its reservoirs) is currently synonymous with *T. mentagrophytes* Type V, the most common genotype of *T. mentagrophytes* isolated from Iranian patients. But the animal reservoirs of this genotype are not well known in Iran and in this investigation, we aimed to determine them.

Methods: A total of 678 skin and hair samples from animals including sheep ($n = 190$), cows ($n = 79$), goats ($n = 9$), camels ($n = 20$), stray and domestic cats ($n = 195$), stray and pet dogs ($n = 146$), horses ($n = 27$), foxes ($n = 2$), hedgehogs ($n = 2$), and poultry ($n = 8$) were subjected to direct microscopy and culture on Mycobiotic agar. Most animals had skin lesions, though some stray cats and dogs were asymptomatic. Molecular identification of dermatophyte cultures was done by ITS-rDNA RFLP. To confirm the RFLP identification, 59 representative isolates from all studied animal species were subjected to ITS-rDNA sequencing. The likelihood for isolation of a specific species or genotype with regard to the type of infected animal was determined using the chi-square test.

Results: We obtained 334 dermatophyte cultures. ITS-RFLP and ITS region sequencing revealed the species *T. verrucosum* ($n = 62$; all from cows), *T. mentagrophytes* Type V (sheep = 95; goat = 6; cat = 1; horse = 2), *T. mentagrophytes* Type II* (cat = 2), *T. mentagrophytes* Type VII (dog = 2), *Microsporium canis* (cats, $n = 94$; dogs, $n = 55$; cow, $n = 1$; horse, $n = 1$), *T. quinqueannum* (fox, $n = 1$), *Nannizzia gypseae* (cats, $n = 5$; dogs, $n = 4$; cow, $n = 1$; horse, $n = 1$), and *N. fulva* (cow, $n = 1$). No dermatophytes were isolated from camels, hedgehogs, and poultry. There was a statistically significant difference in the isolation rate of *T. mentagrophytes* Type V between sampled animals meaning that with a high probability it is isolated from sheep and goats.

Conclusion: Purposive sampling from suspected animals confirmed that sheep are the main animal reservoir of *T. mentagrophytes* Type V, at least in Iran. Further international sequence-based investigations can test our conclusion.

S9.4e

Molecular epidemiology of *Microsporium canis* infection in JapanTakashi Mochizuki¹, Taketoshi Futatsuya¹, Kazushi Anzawa¹, Shigeo Yamada², Akira Shimizu¹¹Kanazawa Medical University, Uchinada Kahoku, Japan, ²Yamada Animal Hospital, Fukui, Japan

S9.4 Free oral presentations (late breaking), September 23, 2022, 4:45 PM - 6:15 PM

Objectives: From a series of epidemiological surveys by the Japanese Society for Medical Mycology, it is estimated that the number of *Microsporium canis* (*M. canis*) infections in Japan has increased in recent years. The purpose of this study was to observe this trend by multilocus microsatellite (MLMT) analysis, a sensitive molecular marker.

Methods: DNA was extracted from 103 strains of *M. canis* isolated between 2017 and 2022 from Japanese patients and pet animals. Using the DNA, PCR targeting six individual microsatellites was performed. The size of each of these amplicons was measured by capillary electrophoresis, and their genotypes were determined from the combinations of their sizes.

Results: A total of 27 genotypes were detected among the 103 strains. Among the 27, 15 had been reported in studies of strains isolated before 2017, whereas 12 were newly determined in the present study. The genotype most frequently detected in the present study was genotype A, being present in 28 of the 103 strains. By geographical region, genotype A was found in strains distributed over a wide area of Japan. Genotype A strains have been isolated from cats purchased at pet shops and/or owners of these pet animals. The highest incidence of genotype A in a study of strains isolated in 2010-2014 was also genotype A. Therefore, a large number of *M. canis* infections originating from pet shops and animal breeders are likely prevalent in Japan today. Furthermore, a relatively large number of strains were identified as genotypes rare or absent in 2010-2014.

Conclusions: The increase in the number of *M. canis* infections in recent years may be the increase in infections of different genotypes, in addition to the base of constant infections by genotype A, by the present MLMT analysis.

S9.5c

***Malassezia*-host interactions and the IL-23/17 axis**

Salomé LeibundGut-Landmann

University of Zurich, Switzerland, Zurich, Switzerland

S9.5 *Malassezia*: pathogenesis and disease, September 23, 2022, 4:45 PM - 6:15 PM

The mycobiome of the skin is dominated by a single fungal genus, *Malassezia*. While *Malassezia* normally exists as a commensal without inflicting disease, the fungus has also been associated with numerous skin disorders ranging from mild conditions such as dandruff or pityriasis versicolor to severe chronic pathologies such as seborrheic or atopic dermatitis. Maintaining stable colonization and preventing pathogenicity of *Malassezia* is key for skin homeostasis. Our understanding of the fungal factors and host mechanisms that, through mutual interactions, promote *Malassezia* commensalism in healthy skin remains incomplete. From studies in humans and mice, we learned that homeostatic immunity against *Malassezia* is characterized by IL-17-producing T cells, including Th17 and γδT17 cells. Recent endeavors start to unravel the cellular and molecular pathways responsible for driving the protective antifungal response in the skin. While *Malassezia*-responsive T cells are non-inflammatory and host-beneficial, they can bear pathogenic potential and thereby be involved in the pathogenesis of inflammatory and allergic skin conditions, as preclinical studies suggest. During my lecture, I will report on recent findings from my lab regarding the role and regulation of the IL-23/IL-17 axis in response to *Malassezia* under normal and diseased skin conditions.

S9.5d

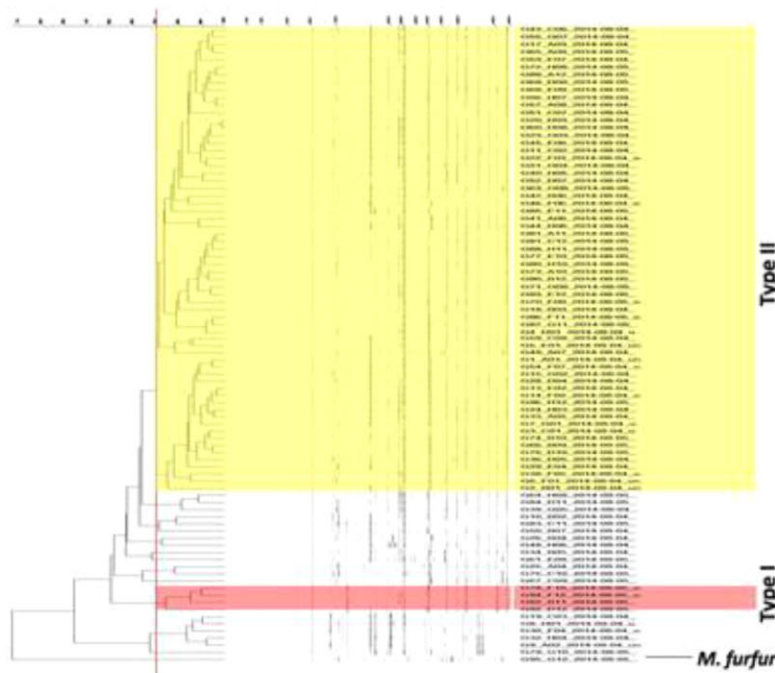
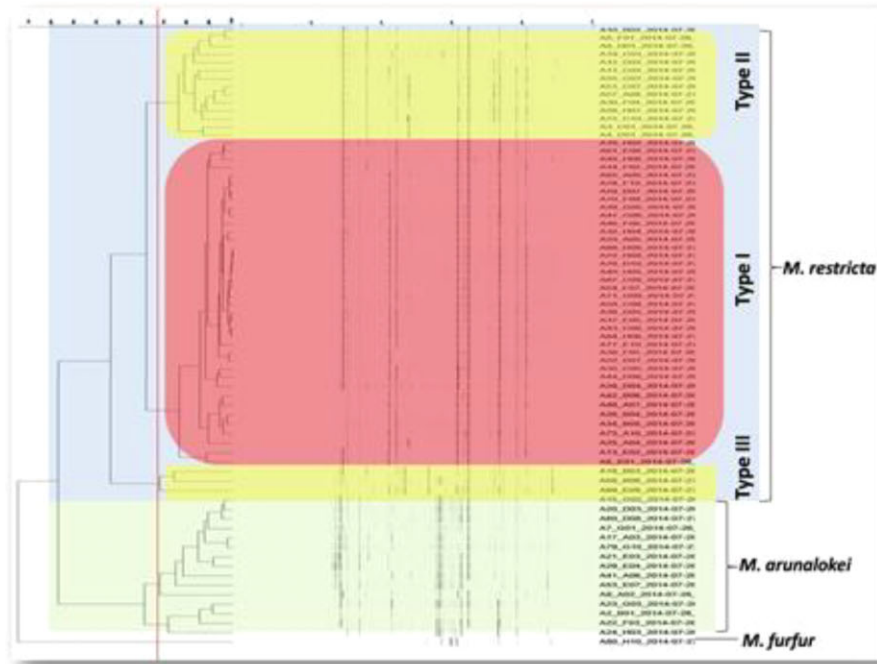
Genotyping of *Malassezia* species from seborrheic dermatitis/dandruff patientsPrasanna Honnavar^{1,2}, Arunaloake Chakrabarti², Sunil Dogra², PVM Lakshmi², Shivaprakash Rudramurthy²¹American University of Antigua College of Medicine (AUACOM), St John, Antigua and Barbuda²Postgraduate Institute of Medical Education and Research (PGIMER), Chandigarh, IndiaS9.5 *Malassezia*: pathogenesis and disease, September 23, 2022, 4:45 PM - 6:15 PM

Objectives: Seborrheic dermatitis/dandruff (SD/D) are common chronic inflammatory skin disorders characterized by recurrent greasy scales with erythema and itchiness. *Malassezia* lobose and *M. restricta* are the predominant agents associated with SD/D. The aim of the study was to differentiate *Malassezia* strains causing SD/D from commensal using a highly discriminatory DNA fingerprinting technique, Fluorescent Amplified Fragment Length Polymorphism (FAFLP).

Methods: A total of 154 (*M. globosa*, $n = 85$; *M. restricta*, $n = 55$; *M. arunalokei*, $n = 14$; standard strains, $n = 3$) isolates from SD/D patients and healthy controls were analyzed using FAFLP. DNA sample was digested with restriction enzymes EcoRI and HindIII, and the fragments were linked to prepared adapters. Pre-selective followed by selective amplification reactions were performed using EcoRI-AC [6-carboxyfluorescein (6-FAM) labeled] and HindIII-T selective primers. The similarity coefficient was determined by Pearson correlation with negative similarities clip to zero. The densitometric curve cluster analysis was performed by unweighted pair group method with arithmetic means using BiNumerics software. The similarity co-efficient of 70% was taken as a cut-off.

Results: *M. restricta* and *M. arunalokei* isolates had a similarity co-efficient of 20%, whereas it was 50% among *M. restricta* and 60% among *M. arunalokei* isolates (Fig. 1). Majority of the isolates ($n = 38.69\%$) clustered to form FAFLP type-I, followed by type-II ($n = 14.25\%$), and type-III ($n = 3.6\%$). All three FAFLP types formed tight clustering among themselves (>80% similarity co-efficient) showing less genetic diversity within each FAFLP type. Type-II clustered strains were isolated from the scalp of SD/D patients ($P < .05$). *M. arunalokei* isolates were clustered into two FAFLP types ($P = .05$). All FAFLP type-I isolates ($n = 10,71\%$) were from the scalp of moderate and severe SD/D patients, whereas all type-II isolates ($n = 4,29\%$) were from nasolabial folds of either SD/D patients or healthy controls. All 11 FAFLP types of *M. globosa* formed very loose structured cluster showing high genetic diversity in intra and inter-FAFLP types (Fig. 2). Majority of the isolates ($n = 63,74\%$) clustered to form FAFLP type-III, followed by type X ($n = 5.6\%$), type-I ($n = 4.5\%$), type-III ($n = 3.3,5\%$), type-IV ($n = 3.3,5\%$), type-V ($n = 2.2\%$), type-VIII ($n = 2.2\%$), and type-VI, VII, IX, XI ($n = 1.1\%$ each). No geographic specific isolate clustering was observed in FAFLP.

Conclusion: *M. restricta* type-II and *M. arunalokei* type-I strains were isolated only from the scalp of moderate to severe forms of SD/D. However, no such severity-specific clustering was observed in *M. globosa*. The results strongly suggest the role of certain genotypes of *M. restricta* and *M. arunalokei* in the causation of SD/D.



S10.1d
Molecular diagnosis and antifungal susceptibility of Colombian clinical isolates of the *Sporothrix* spp complex

Erika Sánchez Cifuentes¹, Martha Úran Álzate¹, Juan Guillermo McEwen Ochoa^{1,2}, Margarita Velasquez^{1,3}, Diana Molina¹, María del Pilar Jiménez Álzate¹

¹Medical Mycology Group, School of Medicine, Universidad de Antioquia, Medellín, Colombia

²Cellular & Molecular Biology Unit, Corporación para las investigaciones Biológicas, Medellín, Colombia

³Dermatological Research Center CIDERM, School of Medicine, Universidad de Antioquia, Medellín, Colombia

S10.1 Antifungal dosing in children and adolescents, September 24, 2022, 10:30 AM - 12:00 PM

Objective: To detect by chitinase PCR and Species-Specific PCR (SS PCR) the DNA of *Sporothrix* spp in fresh tissue and Formalin Fixed Paraffin Embedded (FFPE) tissue from patients with sporotrichosis and to evaluate the susceptibility to antifungal of *Sporothrix* spp isolates obtained from patients diagnosed with sporotrichosis in the Medical Mycology group of the Faculty of Medicine at the University of Antioquia.

Materials & Methods: At the Medical Mycology group service, 26 patients with suspected sporotrichosis were evaluated between 2018 and 2022. Samples of the skin lesions (fresh tissue) were taken for molecular tests and microbiological culture.

Regarding the FFPE tissue, 87 samples stored by different histopathological diagnosis centers from 1976 to 2022 were chosen: 45 samples had a histopathological diagnosis of sporotrichosis, and 42 samples of other diseases with involvement in subcutaneous tissue, were used as controls.

DNAs previously extracted from fresh tissue and FFPE tissue were used to perform chitinase nested PCR and SS nested PCR. The chitinase nested PCR amplifies a 209 bp fragment for the genus *Sporothrix*. For species identification, species-specific primers were used (SS PCR), which amplify a 331 bp sequence for *S. schenckii* s. str. and 243 bp for *S. globosa* of the calmodulin gen. For the SS PCR in tissues, a nested PCR was implemented using the primers CAL1 and CAL2 for the external sequence and the species-specific primers for the internal sequences.

The antifungal susceptibility tests were performed according to the Clinical and Laboratory Standards Institute (CLSI) M27-A3 protocol for yeasts. Six antifungals were used: itraconazole, terbinafine, voriconazole, posaconazole, amphotericin B, and fluconazole.

Results: The culture was positive for *Sporothrix* spp in 15 (58%) patients and the chitinase nested PCR was positive in 14 of these, with a sensitivity of 93% and a specificity of 91%. In 11 patients, both the culture and the chitinase nested PCR were negative.

SS nested PCR was applied to the 14 DNAs with positive chitinase PCR, of which seven were positive for *S. schenckii* s. str. and one for *S. globosa*. For the other six samples, the results of this PCR were negative. The results of these PCR were confirmed by the identification of species from the isolates recovered in culture: 13 were identified as *S. schenckii* s. str. and 1 as *S. globosa*.

Of the 45 FFPE tissue samples with histopathological diagnosis of sporotrichosis, the chitinase PCR was positive for 25 (55%) of these and all FFPE tissue samples were negative for SS nested PCR.

Conclusions: Chitinase nested PCR had a sensitivity of 93% and a specificity of 91% with respect to culture, in samples from fresh tissue. This PCR also has a good performance when it is applied to a good-quality DNA obtained from FFPE tissue, hence, PCR positivity decreased in samples stored for >15 years. The results of the nested SS PCR are encouraging, however, it